

Phenomenology of the Littlest Higgs with T-Parity

Jay Hubisz and Patrick Meade

*Institute for High Energy Phenomenology,
F.R. Newman Laboratory of Elementary Particle Physics,
Cornell University, Ithaca, NY 14853, USA*

hubisz@mail.lepp.cornell.edu, meade@mail.lepp.cornell.edu

Abstract

Little Higgs models offer an interesting approach to weakly coupled electroweak symmetry breaking without fine tuning. The original little Higgs models were plagued by strong constraints from electroweak precision data which required a fine tuning to be reintroduced. An economical solution to this problem is to introduce a discrete symmetry (analogous to R-parity of SUSY) called T-parity. T-parity not only eliminates most constraints from electroweak precision data, but it also leads to a promising dark matter candidate. In this paper we investigate the dark matter candidate in the littlest Higgs model with T-parity. We find bounds on the symmetry breaking scale f as a function of the Higgs mass by calculating the relic density. We begin the study of the LHC phenomenology of the littlest Higgs model with T-parity. We find that the model offers an interesting collider signature that has a generic missing energy signal which could “fake” SUSY at the LHC. We also investigate the properties of the heavy partner of the top quark which is common to all littlest Higgs models, and how its properties are modified with the introduction of T-parity. We include an appendix with a list of Feynman rules specific to the littlest Higgs with T-parity to facilitate further study.

1 Introduction

Within the next decade the mechanism responsible for electroweak symmetry breaking (EWSB) will hopefully be revealed by the LHC. For theoretical physicists this is a time at which many attempt to conjecture every possibility before experimental data ultimately chooses the correct one (or at least narrows the list). The standard paradigm for weakly coupled EWSB is the Higgs mechanism, however in the Standard Model (SM) there are quadratically divergent diagrams which contribute to the Higgs mass. If new physics to cut off the quadratic divergences to the Higgs mass does not occur at approximately the TeV scale, the SM will be a finely tuned theory. As long as one takes naturalness as a guide for model building this implies that there should be new physics at the TeV scale associated with the physics of EWSB. For two decades the standard for new physics at the TEV scale, which cancels the quadratic divergences of the SM Higgs, was supersymmetry. With the turn on of the LHC drawing near there have recently been many attempts at coming up with viable alternatives to supersymmetry. The alternative that will be focused on in this paper will be the little Higgs mechanism [1].

The origin of the little Higgs idea dates back almost as far as supersymmetry to the papers of Georgi et al. [2, 3] that attempted to realize the Higgs as a pseudo-Goldstone boson (PGB). These original papers were unsuccessful due to the fact that they reintroduced a fine tuning to keep the symmetry breaking scale that generates the Goldstone separate from the electroweak scale. The new mechanism that makes the Higgs “little” in the current reincarnation of the PGB idea is collective symmetry breaking [1]. Collective symmetry breaking protects the Higgs by several symmetries under each of which the Higgs is an exact Goldstone. Only if the symmetries are broken collectively, i.e. by more than one coupling in the theory, can the Higgs pick up a contribution to its mass and hence all one loop quadratic divergences (which involve one coupling alone) to the Higgs mass are avoided.

The generic structure of little Higgs models [4, 5, 6, 7, 8, 9, 10, 11] is a global symmetry broken at a scale f which is around a TeV. At the scale f there are new gauge bosons, scalars, and fermions responsible for cancelling the one loop quadratic divergences to the Higgs mass from SM particles (for a brief review of the gauge and global symmetries of most little Higgs models see [12]). Even though there are no direct experimental signatures that guide model building beyond the SM, there are many indirect constraints that a model of new physics must satisfy. Whenever one tries to introduce new particles around the TeV scale which couple to SM particles there is usually a tension with precision EW measurements which typically favor the scale of new physics to be ~ 5 -10 TeV. This tension between having to introduce new physics at the TeV scale for naturalness, and EW precision tests (EWPT) preferring the scale of new physics to be a factor of ~ 10 higher is the so called “little” hierarchy problem. The original little Higgs models unfortunately did not relieve the tension caused by EWPT. The scale f had to be raised significantly above a TeV, which reintroduced a fine tuning to the Higgs mass [13, 14, 15]. New little

Higgs models [8, 10] were introduced with much larger symmetry structures that could incorporate a custodial $SU(2)$ symmetry which then ameliorated most of the problems from EW constraints. In keeping with the idea of looking for alternatives to SUSY a more economical solution to the “little” hierarchy problem was proposed in [16, 17].

In trying to find alternatives to the MSSM one should examine the model critically to find what are the keys to its success. The MSSM is unarguably the most theoretically well motivated extension of the SM, including a stable hierarchy between the weak and Planck scales, as well as gauge coupling unification. However the key to the MSSM is R -parity, a discrete symmetry introduced by hand, without which the MSSM would be ruled out by experiment. The motivation for R -parity is normally to forbid operators that would lead to rapid proton decay, but with the introduction of R -parity it also forbids dangerous four-fermion operators and contributions to Z -pole observables. The R -parity also governs the signatures of the MSSM in colliders since the conservation of R -parity requires all R -odd particles to be pair produced. If the lightest parity odd particle in the MSSM is neutral, the signal in detectors will be missing energy.

If the leading candidate for new physics at the TeV scale relies upon a discrete symmetry to be phenomenologically acceptable it is quite plausible that its alternatives could incorporate a discrete symmetry as well [16, 17]. Introducing a discrete symmetry called “T-parity” into little Higgs models was done first in [17], and applied to other little Higgs models in [18, 19]. T-parity is a natural symmetry of most little Higgs models where SM particles are even under the symmetry while most of the new particles at the TeV scale are odd. Most of the constraints from EWPT on little Higgs models [13, 14, 15] come from tree level mixing of heavy and light mass eigenstates which T-parity forbids. T-parity therefore solves the little hierarchy problem for the models in which it can be implemented [18]. T-parity also has a further benefit, if the lightest parity odd particle is neutral and T-parity is conserved it will be a candidate for a dark matter WIMP (just as R-parity provides a candidate WIMP under the same circumstances for supersymmetry).

In this paper we will study the phenomenology of the littlest Higgs model [4] with the addition of T-parity [18, 19]. There have been many studies of the phenomenology of the littlest Higgs model [20, 21, 22]; however with the introduction of T-parity most of these studies do not apply since the T-odd particles can not be singly produced. We begin with reviewing the littlest Higgs model with T-parity in Section 2. It turns out that there are several different approaches to incorporating T-parity into the littlest Higgs model and we discuss in Section 2.2 how most reduce to a similar low energy effective spectrum that we study. In Section 3 we investigate the phenomenology of the dark matter candidate in the littlest Higgs model which is a heavy neutral gauge boson. In Section 4 we explore the discovery possibilities for the littlest Higgs with T-parity at the LHC. In Appendix A, we discuss four fermion operators in the model that we chose to study. In Appendix B we list Feynman rules for the littlest Higgs with T-parity to facilitate further study of the model.

2 Review of the “Littlest” Higgs Model with T-Parity

There are currently three known ways to implement T-parity in the littlest Higgs model [18, 19]. The first approach uses the technology of Callan, Coleman, Wess, and Zumino (CCWZ) [18, 23], where the model is almost identical to the original littlest Higgs model except for the fermion sector. The other approaches [19] to implementing T-parity in the littlest Higgs rely on enlarging the global and gauge symmetry structure but are similar to the CCWZ littlest Higgs model with T-parity in the low energy limit. For the sake of studying a concrete model we will first discuss in detail the CCWZ approach that the calculations in this paper are based upon. We will then discuss the other ways to implement T-parity and how the low energy phenomenology of all three implementations are approximately the same.

2.1 Littlest Higgs with T-parity

The original littlest Higgs model was based on a non-linear σ model describing an $SU(5)/SO(5)$ symmetry breaking [4] and serves as the starting point for including T-parity [18]. The symmetry breaking can be thought of as originating from a vacuum expectation value (VEV) of a symmetric tensor of the $SU(5)$ global symmetry. A convenient basis for this breaking is characterized by the direction Σ_0 for the VEV of the form

$$\Sigma_0 = \begin{pmatrix} & & & & 1 \\ & & & & & 1 \\ & & & 1 & & \\ & & 1 & & & \\ 1 & & & & & \\ & 1 & & & & \end{pmatrix}. \quad (2.1)$$

The Lie algebra made up of the broken generators, X^a , and unbroken generators, T^a , has an automorphism where $T^a \rightarrow T^a$ and $X^a \rightarrow -X^a$, which can be expressed as $\tau^a \rightarrow -\Sigma_0(\tau^a)^T\Sigma_0$ for any generator τ_a . This Z_2 automorphism of the symmetric space $SU(5)/SO(5)$ will be a useful guide in implementing T-parity. The Goldstone fluctuations are described by the pion fields $\Pi = \pi^a X^a$. The non-linear sigma model field is then

$$\Sigma(x) = e^{i\Pi/f}\Sigma_0 e^{i\Pi^T/f} = e^{2i\Pi/f}\Sigma_0. \quad (2.2)$$

where f is the value of the VEV that accomplishes the breaking. An $[SU(2) \times U(1)]^2$ subgroup of the $SU(5)$ global symmetry is gauged, where the generators of the gauged

symmetries are given by

$$\begin{aligned}
Q_1^a &= \begin{pmatrix} \sigma^a/2 & 0 & 0 \\ 0 & 0 & 0 \\ 0 & 0 & 0 \end{pmatrix}, & Y_1 &= \text{diag}(3, 3, -2, -2, -2)/10 \\
Q_2^a &= \begin{pmatrix} 0 & 0 & 0 \\ 0 & 0 & 0 \\ 0 & 0 & -\sigma^{a*}/2 \end{pmatrix}, & Y_2 &= \text{diag}(2, 2, 2, -3, -3)/10,
\end{aligned} \tag{2.3}$$

where σ^a are the Pauli σ matrices. The Q^a 's are 5×5 matrices written in terms of 2×2 , 1, and 2×2 blocks. The vacuum breaks the $[SU(2) \times U(1)]^2$ gauge symmetry down to the diagonal subgroup, giving one set of $[SU(2) \times U(1)]$ gauge bosons masses of order f , while the other set are left massless, and are identified as the $SU(2)_L \times U(1)_Y$ gauge fields of the standard model. The Goldstone boson matrix Π is given by

$$\Pi = \begin{pmatrix} 0 & \frac{H}{\sqrt{2}} & \Phi \\ \frac{H^\dagger}{\sqrt{2}} & 0 & \frac{H^T}{\sqrt{2}} \\ \Phi^\dagger & \frac{H^*}{\sqrt{2}} & 0 \end{pmatrix}, \tag{2.4}$$

where H is the little Higgs doublet $(h^+, h)^T$ and Φ is a complex triplet under $SU(2)_L$ which forms a symmetric tensor Φ_{ij} with components $\phi^{++}, \phi^+, \phi^0$ and a pseudoscalar ϕ^P as defined in [21]. ϕ^0 and ϕ^P are both real scalars. The Goldstone bosons which are eaten to become the longitudinal modes of the partners of the standard model gauge fields are set to zero in the pion matrix, as we have gone to unitary gauge.

The underlying idea for implementing T-parity is to assign all non-SM particles odd parity, and all SM particles even parity, thus avoiding tree level constraints from EWPT. It turns out that there will be one case in which this assignment is not possible when we discuss the top quark sector of the model, however for the gauge and scalar sectors all non-SM particles are T-odd. To implement T-parity in the gauge sector one notices that the Σ_0 VEV separates the gauged generators into a broken set $\{Q_1^a - Q_2^a, Y_1 - Y_2\}$ and an unbroken set $\{Q_1^a + Q_2^a, Y_1 + Y_2\}$ of generators. Using the action of the Z_2 inner automorphism discussed earlier, $T^a \rightarrow T^a$ for unbroken generators, and $X^a \rightarrow -X^a$ for broken generators, a natural action of T-parity on the gauge fields is defined as

$$A_1 \leftrightarrow A_2, \tag{2.5}$$

where A_1, A_2 are the gauge fields corresponding to the $[SU(2) \times U(1)]_1$ and $[SU(2) \times U(1)]_2$ gauge groups, respectively. The action for T-parity in the scalar sector is defined as

$$\Pi \rightarrow -\Omega \Pi \Omega, \tag{2.6}$$

where $\Omega = \text{diag}(1, 1, -1, 1, 1)$. Ω is introduced to give the Higgs positive parity while keeping the triplet odd. From the transformation of Π we can also write the transformation law for Σ under T-parity

$$\Sigma \rightarrow \Sigma_0 \Omega \Sigma^\dagger \Omega \Sigma_0 \equiv \tilde{\Sigma}. \tag{2.7}$$

The kinetic term of the non-linear σ model field Σ in the littlest Higgs is

$$\frac{f^2}{8} \text{Tr} D_\mu \Sigma (D^\mu \Sigma)^\dagger, \quad (2.8)$$

where

$$D_\mu \Sigma = \partial_\mu \Sigma - i \sum_j [g_j W_j^a (Q_j^a \Sigma + \Sigma Q_j^{aT}) + g'_j B_j (Y_j \Sigma + \Sigma Y_j)], \quad (2.9)$$

with $j = 1, 2$. The kinetic terms for the sigma field and gauge bosons are invariant under T-parity as written down originally in the littlest Higgs model with the additional proviso that $g_1 = g_2 = \sqrt{2}g$ and $g'_1 = g'_2 = \sqrt{2}g'$. Since T-parity exchanges the gauge fields (2.5), the gauge couplings must be equal for the Lagrangian to be invariant. We identify g and g' with the SM $SU(2)$ and $U(1)_Y$ gauge couplings respectively.

In the gauge sector before EWSB there is a linear combination of gauge bosons that acquire a mass of order f from (2.8),

$$\begin{aligned} W_H^a &= \frac{1}{\sqrt{2}}(W_1^a - W_2^a), & M_{W_H^a} &= gf, \\ B_H &= \frac{1}{\sqrt{2}}(B_1 - B_2), & M_{B_H} &= \frac{g'}{\sqrt{5}}f, \end{aligned} \quad (2.10)$$

while the linear combinations

$$W_L^a = \frac{1}{\sqrt{2}}(W_1^a + W_2^a), \quad B_L = \frac{1}{\sqrt{2}}(B_1 + B_2), \quad (2.11)$$

remain massless and are identified with the SM gauge bosons. From the T-parity transformation (2.5) the heavy gauge bosons are odd under T-parity while the SM gauge bosons are even. After EWSB the VEV of the Higgs, $\langle H \rangle^T = (0, v/\sqrt{2})$, will shift the mass eigenstates in the heavy gauge boson sector. The new mass eigenstates in the neutral heavy sector will be a linear combination of the W_H^3 and the B_H gauge bosons, producing an A_H and a Z_H . The mixing angle introduced into the neutral heavy sector by EWSB will be of order v^2/f^2 :

$$\sin \theta_H \approx \frac{5gg'}{4(5g^2 - g'^2)} \frac{v^2}{f^2}. \quad (2.12)$$

The new heavy neutral mass eigenstates are given by

$$\begin{aligned} Z_H &= \sin \theta_H B_H + \cos \theta_H W_H^3, & M_{Z_H}^2 &= g^2 f^2 - \frac{g^2 v^2}{4} \\ A_H &= \cos \theta_H B_H - \sin \theta_H W_H^3, & M_{A_H}^2 &= \frac{g'^2 f^2}{5} - \frac{g'^2 v^2}{4} \end{aligned} \quad (2.13)$$

while a set of heavy charged gauge bosons can be written as

$$W_H^\pm = \frac{1}{\sqrt{2}}(W_H^1 \mp iW_H^2), \quad M_{W_H^\pm}^2 = g^2 f^2 - \frac{g^2 v^2}{4}. \quad (2.14)$$

In the scalar sector from the T-parity transformation (2.6) one can see that the Higgs doublet has positive parity under this transformation, and that the $SU(2)_L$ triplet Φ has

odd parity. We will briefly recall that in a little Higgs model, EWSB is generated radiatively through the Coleman-Weinberg potential. The difference from [4] in this sector with the addition of T-parity is that the coupling $H\Phi H$ is forbidden by T-parity. The absence of the $H\Phi H$ coupling forbids a dangerous non-zero triplet VEV[13, 15] after EWSB. The mass of Φ can be related to the mass of the Higgs from the Coleman-Weinberg potential [21] to give

$$m_\Phi^2 = \frac{2m_H^2 f^2}{v^2}, \quad (2.15)$$

where all components of the triplet are degenerate at the order we are examining.

In summary, the implementation of T-parity for the gauge sector has essentially decoupled the light and heavy sectors by setting $g_1 = g_2$ and $g'_1 = g'_2$. T-parity has also forbidden the VEV of the triplet Φ . Most constraints from EWPT on the original littlest Higgs [13, 14, 15] vanish in this limit.

To fully implement T-parity in a consistent way we must now turn our attention to the fermion sector. We would like to introduce SM fermions that transform linearly under the gauge symmetries to avoid large contributions to four fermion operators that would require the scale f to be large [19]. Since T-parity exchanges $SU(2)_1$ and $SU(2)_2$ one must introduce two doublets ψ_1 , and ψ_2 , which transform linearly under $SU(2)_1$ and $SU(2)_2$ respectively. These doublets are mapped into each other under the action of T-parity. To obtain the SM at low energy we would like to give an f scale mass to the T-odd linear combination of these doublets. In giving mass to only the T-odd linear combination, at this stage one should introduce a “mirror” fermion with odd parity and write down a mass term with the T-odd linear combination of ψ_1 and ψ_2 [19]. Since T-parity exchanges the two $SU(2)$'s, to avoid introducing an additional copy of the mirror fermion, it must have a non-linear symmetry transformation.

We will now explain in detail how to make a gauge invariant term that only gives mass to the T-odd linear combination of ψ_1 and ψ_2 . For those readers only interested in the phenomenology it is not crucial to understand where in the end the expression (2.20) comes from, but it is important to note that there will be additional interactions apart from just mass terms in (2.20). A set of mirror fermions Ψ' is introduced in a complete multiplet of $SO(5)$, whose transformation under $SU(5)$ is non-linear. The mirror fermions must be introduced in a complete multiplet in order to eliminate potential quartic divergences in the Higgs mass [18]. In order to give this Ψ' multiplet interactions with other fields which obey linear transformation laws, we introduce a field $\xi = e^{i\Pi/f}$. This technology, for those readers familiar with it, is reminiscent of introducing baryons in a nonlinear chiral $SU(3)_L \times SU(3)_R$ model [24]. In terms of ξ , the field Σ can be expressed as $\Sigma = \xi^2 \Sigma_0$. From the linear transformation of Σ , we infer that the field ξ has the following transformation under a global $SU(5)$ rotation V :

$$\Sigma \rightarrow V\Sigma V^T \quad \Rightarrow \quad \xi \rightarrow U\xi\Sigma_0 V^T \Sigma_0 = V\xi U^\dagger \quad (2.16)$$

where U takes values in the Lie algebra of the unbroken $SO(5)$ subgroup, and is a function

of both V and the pion fields. It is this same U under which the Ψ' multiplet transforms:

$$\Psi' \rightarrow U\Psi'. \quad (2.17)$$

The fermion doublets ψ_1, ψ_2 can be embedded into incomplete representations Ψ_1, Ψ_2 of $SU(5)$, and the field content can be expressed as follows:

$$\Psi_1 = \begin{pmatrix} \psi_1 \\ 0 \\ 0 \end{pmatrix} \quad \Psi_2 = \begin{pmatrix} 0 \\ 0 \\ \psi_2 \end{pmatrix} \quad \Psi' = \begin{pmatrix} \tilde{\psi}' \\ \chi' \\ \psi' \end{pmatrix} \quad (2.18)$$

where χ' is a singlet and $\tilde{\psi}'$ is a doublet under $SU(2)_2$. The transformation laws for Ψ_1 and Ψ_2 are as follows:

$$\Psi_1 \rightarrow V^*\Psi_1 \quad \Psi_2 \rightarrow V\Psi_2 \quad (2.19)$$

The action of T-parity on the multiplets takes $\Psi_1 \leftrightarrow -\Sigma_0\Psi_2$ and $\Psi' \rightarrow -\Psi'$. One can now write down a Yukawa-type interaction to give masses to the mirror fermions,

$$\kappa f (\bar{\Psi}_2 \xi \Psi' + \bar{\Psi}_1 \Sigma_0 \Omega \xi^\dagger \Omega \Psi'), \quad (2.20)$$

which is invariant under a global $SU(5)$ rotation, and also under the action of T-parity. From (2.20) one fermion doublet $\psi_H = \frac{1}{\sqrt{2}}(\psi_1 + \psi_2)$ acquires a mass κf , while the other combination $\psi_{SM} = \frac{1}{\sqrt{2}}(\psi_1 - \psi_2)$ remains massless and is identified with the SM doublets. To give masses to the remaining fields χ' and $\tilde{\psi}'$ one must introduce additional fermions χ and $\tilde{\psi}$ along with another singlet $\tilde{\chi}$ which occupy a spinor representation of $SO(5)$, S , and then introduce Dirac mass terms for these fields.

After introducing the Yukawa coupling (2.20) which gives the mirror fermions mass we need to introduce kinetic terms for the fermions in this model. Since Ψ_1 and Ψ_2 transform linearly, their kinetic terms are straightforward to write down:

$$\mathcal{L}_{kin} \supset \bar{\Psi}_1 \bar{\sigma}^\mu D_\mu^1 \Psi_1 + \bar{\Psi}_2 \bar{\sigma}^\mu D_\mu^2 \Psi_2, \quad (2.21)$$

where

$$D_\mu^1 = \partial_\mu - i\sqrt{2}gQ_1^a W_1^a - i\sqrt{2}g'Y_1^{(\Psi_1)} B_{1\mu} - i\sqrt{2}g'Y_2^{(\Psi_1)} B_{2\mu}, \quad (2.22)$$

$$D_\mu^2 = \partial_\mu + i\sqrt{2}g(Q_2^a)^T W_1^a - i\sqrt{2}g'Y_1^{(\Psi_2)} B_{1\mu} - i\sqrt{2}g'Y_2^{(\Psi_2)} B_{2\mu}, \quad (2.23)$$

and the $U(1)$ charges $Y_i^{(\Psi_j)}$ are given in Table 1 which will can be determined from gauge invariance of the Yukawa couplings and T-parity. Re-expressing (2.21) in terms of the mass eigenstates found from (2.20) one obtains

$$\mathcal{L}_{kin} \supset \bar{\psi}_{SM} \bar{\sigma}^\mu D_\mu^L \psi_{SM} + \bar{\psi}_H \bar{\sigma}^\mu D_\mu^L \psi_H, \quad (2.24)$$

which contains the usual kinetic terms for the SM doublet fermions where D_μ^L is the usual SM covariant derivative, as well as kinetic terms for the heavy fermions. In addition to the standard kinetic terms in (2.24) there are interaction terms of the form

$$c\bar{\psi}_{SM}\bar{\sigma}^\mu V_{H\mu}\psi_H, \quad (2.25)$$

where c is a gauge coupling and V_H is a heavy gauge boson. These new interactions between heavy and light fields come from expressing (2.21) in mass eigenstates. To write down an invariant kinetic term for the Ψ' field we must make use of the ξ field in the following way

$$\bar{\Psi}'\bar{\sigma}^\mu(\partial_\mu + \xi^\dagger D_\mu\xi + \xi D_\mu^T\xi^\dagger)\Psi', \quad (2.26)$$

where

$$\begin{aligned} D_\mu &= \partial_\mu - icV_L Q_V - icV_H Q_A, \\ D_\mu^T &= \partial_\mu - icV_L Q_V + icV_H Q_A. \end{aligned} \quad (2.27)$$

D_μ^T is the T-parity transformed covariant derivative. One can write down a similar kinetic term for the spinor field S by expressing the covariant derivatives in Eq. (2.27) in the spinor representation of $SO(5)$. There are dangerous four fermion operators arising at the one loop level which the T-odd partners of the standard model left handed doublets serve to cut off, thus these fermions cannot be taken to be arbitrarily heavy. We discuss this in more detail in Appendix A. For the purposes of studying a simpler, and model independent phenomenology, we neglect these fermions in this paper, leaving their study for future work.

In order to avoid dangerous contributions to the Higgs mass from one loop quadratic divergences, the third generation Yukawa sector must be modified so that it incorporates the collective symmetry breaking pattern of [4]. In order to do this, the Ψ_1 and Ψ_2 multiplets for the third generation must be completed to representations of the $SU(3)_1$ and $SU(3)_2$ subgroups of the full $SU(5)$. These are

$$Q_1 = \begin{pmatrix} q_1 \\ t'_1 \\ 0 \end{pmatrix} \quad Q_2 = \begin{pmatrix} 0 \\ t'_2 \\ q_2 \end{pmatrix}, \quad (2.28)$$

where Q_1 and Q_2 obey the same transformation laws under T-parity and the $SU(5)$ symmetry as do Ψ_1 and Ψ_2 . It should be noted that the quark doublets are embedded such that

$$q_i = -i\sigma_2 \begin{pmatrix} t_i \\ b_i \end{pmatrix}. \quad (2.29)$$

One must also introduce additional singlets t'_{1R} and t'_{2R} which transform under T-parity as

$$t'_{1R} \leftrightarrow -t'_{2R} \quad (2.30)$$

so the top sector masses can be generated in the following T-parity invariant way

$$\begin{aligned} \mathcal{L}_t = & \frac{1}{2\sqrt{2}}\lambda_1 f \epsilon_{ijk} \epsilon_{xy} [(\bar{Q}_1)_i (\Sigma)_{jx} (\Sigma)_{ky} - (\bar{Q}_2 \Sigma_0)_i (\tilde{\Sigma})_{jx} (\tilde{\Sigma})_{ky}] u_{3R} \\ & + \lambda_2 f (\bar{t}'_1 t'_{1R} + \bar{t}'_2 t'_{2R}) + h.c. \end{aligned} \quad (2.31)$$

We point out that this is a slightly different implementation of the top Yukawa coupling than in [19]; T-parity and gauge invariance require the couplings of t'_1 and t'_2 to be equal and leads to new phenomenology for the heavy top quarks. This Yukawa term generates a mass for the top quark given by

$$m_{\text{top}} = \frac{\lambda_1 \lambda_2 v}{\sqrt{\lambda_1^2 + \lambda_2^2}}, \quad (2.32)$$

while the T-even combination of t'_1 and t'_2 has mass

$$m_{t'_+} = \sqrt{\lambda_1^2 + \lambda_2^2} f, \quad (2.33)$$

and the T-odd combination has mass

$$m_{t'_-} = \lambda_2 f, \quad (2.34)$$

with $t'_\pm = \frac{1}{\sqrt{2}}(t'_1 \mp t'_2)$. The T-odd combination of the q_1 and q_2 doublets obtains a mass through a Yukawa identical to Equation (2.20). The other two generations of up-type quarks acquire their mass through similar terms, though with the t' quarks missing from the Q_1 and Q_2 multiplets since the Yukawa couplings are small and one does not have to worry about quadratic divergences. Requiring that the top-sector Yukawa term be gauge invariant determines the $U(1)$ charges of the fermions up to one degree of freedom, which is then fixed by imposing T-parity. The resulting charges are given in Table 1.

q_1	$(\mathbf{2}, 1/30; \mathbf{1}, 2/15)$	q_2	$(\mathbf{1}, 2/15; \mathbf{2}, 1/30)$
t'_1	$(\mathbf{1}, 8/15; \mathbf{1}, 2/15)$	t'_2	$(\mathbf{1}, 2/15; \mathbf{1}, 8/15)$
t'_{1R}	$(\mathbf{1}, 8/15; \mathbf{1}, 2/15)$	t'_{2R}	$(\mathbf{1}, 2/15; \mathbf{1}, 8/15)$
u_{3R}	$(\mathbf{1}, 1/3; \mathbf{1}, 1/3)$	d_R	$(\mathbf{1}, -1/6, \mathbf{1}, -1/6)$
l_1	$(\mathbf{2}, -1/5; \mathbf{1}, -3/10)$	l_2	$(\mathbf{1}, -3/10, \mathbf{1}, -1/5)$
e_R	$(\mathbf{1}, -1/2; \mathbf{1}, -1/2)$		

Table 1: The $[SU(2)_1 \times U(1)_1] \times [SU(2)_2 \times U(1)_2]$ quantum numbers of the fermion fields that are required to make Eqns. (2.20),(2.31), and (2.35) gauge invariant.

We also need to construct a Yukawa interaction which gives the down-type quarks a mass after electroweak symmetry breaking. The following term accomplishes this:

$$\mathcal{L}_d = \frac{1}{4} \lambda_d f \epsilon_{ij} \epsilon_{xy} [(\bar{\Psi}'_2)_x (\Sigma)_{3i} (\Sigma)_{jy} - (\bar{\Psi}'_1 \Sigma_0)_x (\tilde{\Sigma})_{3i} (\tilde{\Sigma})_{jy}] d_R + h.c. \quad (2.35)$$

The doublets are embedded in Ψ'_1 and Ψ'_2 such that

$$\Psi'_1 = \begin{pmatrix} -i\sigma_2 q_1 \\ 0 \\ 0 \end{pmatrix} \quad \Psi'_2 = \begin{pmatrix} 0 \\ 0 \\ -i\sigma_2 q_2 \end{pmatrix}, \quad (2.36)$$

and they transform under $SU(5)$ as $\Psi'_1 \rightarrow V\Psi'_1$, and $\Psi'_2 \rightarrow V^*\Psi'_2$. The lepton Yukawas can be taken to be identical to Equation (2.35).

The final spectrum that we consider has some important features that we briefly summarize. In Figure 1 we give an example spectrum for a typical choice of model parameters. The lightest new particle introduced in this model is the A_H . The array of scalars coming from the $SU(2)_L$ triplet can be either lighter than, or more massive than the W_H and Z_H gauge bosons, depending on the values of f and m_H . For smaller m_H and f smaller than 1 TeV, the scalar triplet is lighter than these gauge fields, but for larger f and m_H the triplet is in fact more massive. A useful parameter that we will use to discuss the new fermions, t'_+ and t'_- , is

$$s_\lambda \equiv \frac{\lambda_2}{\sqrt{\lambda_1^2 + \lambda_2^2}} = \frac{m_{t'_-}}{m_{t'_+}}. \quad (2.37)$$

One thing to notice in particular is that the t'_- fermion is always lighter than the t'_+ . This will lead to novel phenomenology for the t'_+ that was not present before the introduction of T-parity.

2.2 Alternative implementations of T-parity

We will now turn our discussion to other implementations of T-parity [19] in the littlest Higgs, to give credence to why we will study the phenomenology of only the model described in Section 2.1 in detail. In the original 3-site moose model of T-parity described in [17], three copies of $SU(2) \times U(1)$ were gauged, one at each site. In this model, T-parity was realized as a symmetry exchanging two of the sites, while the third site was neutral under the action of T-parity. This kind of set up enabled fermions to be introduced in linear representations which naturally avoids the constraints imposed when SM fermions have non-linear gauge transformations [19]. One can come up with an analogous set up to the three-site moose model with a littlest Higgs structure [19] by enlarging the global symmetry of the littlest Higgs and gauging a third copy of $SU(2) \times U(1)$. In [19] the specific implementations of this idea were accomplished by enlarging the global structure $SU(5)/SO(5)$ to $(SU(5) \times G_r)/SO(5)$ where G_r was either $SO(5)$ or $SU(5)$. The same generators as in (2.3) are gauged along with an additional $SU(2) \times U(1)$

$$Q_r^a = \begin{pmatrix} \sigma^a/2 & 0 & 0 \\ 0 & 0 & 0 \\ 0 & 0 & -\sigma^{a*}/2 \end{pmatrix}, \quad Y_r = \text{diag}(1, 1, 0, -1, -1)/2. \quad (2.38)$$

Example Spectrum of the Littlest Higgs with T-parity

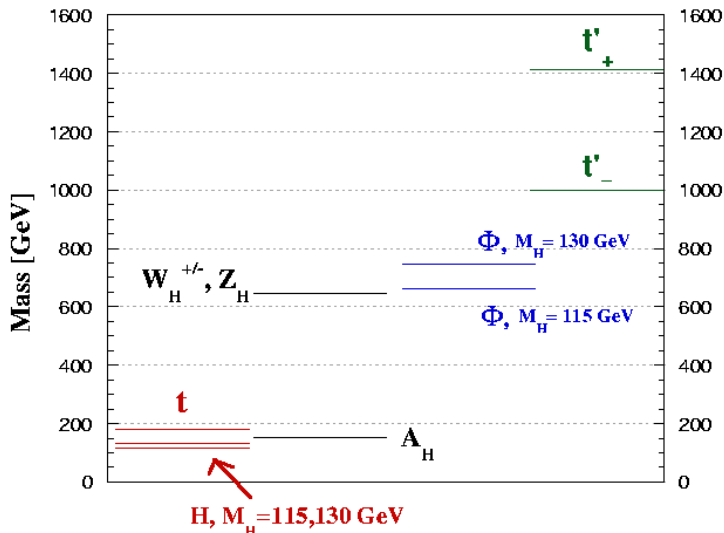


Figure 1: We plot a sample spectrum for the littlest Higgs with T-parity. The top quark mass and two values of the Higgs mass are plotted as a reference. The spectrum of heavy particles is plotted for $f = 1$ TeV. The Φ mass is plotted for two different values of the Higgs mass, $M_H = 115, 130$ GeV. A value of $s_\lambda = \frac{1}{\sqrt{2}}$ is used to determine the masses of t'_+ and t'_- .

One should immediately note that in this class of models with a third set of gauge groups which is neutral under T-parity, there will be new T-even heavy gauge bosons. In addition, there will also be T-even heavy scalars. Having T-even heavy gauge bosons and scalars is a rather dangerous prospect given that EWPT normally require the scale f to be large, which reintroduces a fine tuning [13, 15]. In this class of model with three sets of $SU(2) \times U(1)$ gauge groups the problem of raising the scale f is avoided by taking the gauge couplings g_r of the third set to be $g_r \sim 4\pi$, which decouples the heavy T-even gauge bosons. The new heavy T-even scalars can be decoupled by introducing strongly coupled plaquette operators which raise the scalar masses to $\mathcal{O}(10 \text{ TeV})$.

If one is willing to take the limits just described to avoid the constraints of EWPT, the resulting theory will be identical in the gauge and scalar sectors (around the TeV scale and below) to the littlest Higgs with T-parity discussed in Section 2.1. The only difference between the implementation discussed in Section 2.1 and the $(SU(5) \times G_r)/SO(5)$ models arises in the fermion sector. All of the implementations of the fermion sector have a mirror fermion type implementation of the SM fermions (e.g. (2.20)). The type of Σ or ξ fields available in the particular model [19] will dictate the number of fermions required to write down a heavy Yukawa to lift the mass of one set of fermions as in (2.20). One thing that must be pointed out is that in the top sector, all three types of littlest Higgs with T-parity

have the same spectrum. Each model contains a T-odd and T-even partner of the top quark at the TeV scale where all implementations share the same couplings (2.31). In the heavy Yukawa sector as mentioned before, the number of fermions is different in the three implementations but it is important to point out that the masses of the new fermions are constrained. In the little Higgs models with T-parity, generically one requires some of the mirror fermion doublets to have $\mathcal{O}(\text{TeV})$ masses or lower to avoid constraints on four fermion operators.

In analyzing the phenomenology of the littlest Higgs with T-parity we use the model outlined in Section 2.1 for the following reason. Since the CCWZ implementation has an identical scalar and gauge sector at around a TeV (because of the EW constraints on the two other implementations), one does not have to rely on strong coupling and one captures much of the interesting phenomenology that does not rely on the details of the fermion spectrum. Since the top Yukawa sector of the model is identical in all three implementations we will capture its phenomenology in any of the models. In this paper we will choose to ignore all T-odd heavy fermions except for the t'_- . Further analysis of the fermion sector would be an interesting future project to see the implications of more T-odd fermions at the TeV scale, both in collider studies, and in electroweak precision.

3 The A_H as a dark matter candidate

If we require that T-parity be an exact, or nearly exact, symmetry, the lightest new particle introduced is stable. While EWP does not require such a large suppression of the tree level operators, it is interesting to pose the question of whether T-parity is part of a more fundamental symmetry arising from the ultraviolet completion of the little Higgs mechanism. If this particle is also neutral, it provides a promising candidate for WIMP dark matter. This particle will be in equilibrium with the thermal bath at early times in the history of the universe, being pair produced in collisions of lighter standard model particles, and annihilating via the same channels. As the universe cools however, these processes will fall out of equilibrium, and the number density of the lightest parity odd particle (LPOP) will begin to decrease. This happens until the rate of expansion of the universe overtakes the annihilation rate, at which point the abundance of the LPOP will freeze out. From this point on the relic abundance of the LPOP will simply follow the expansion rate. This process is described by a Boltzmann equation

$$\frac{dn_\chi}{dt} + 3Hn_\chi = -\langle\sigma_A v\rangle [n_\chi^2 - (n_\chi)_{\text{eq}}^2], \quad (3.39)$$

where $\langle\sigma_A v\rangle$ is the thermally averaged annihilation coefficient for the WIMP χ . H is the Hubble constant, n_χ is the number density of the WIMP in the thermal bath, and $(n_\chi)_{\text{eq}}$ is the equilibrium number density. The annihilation cross section is given by

$$\sigma_A = \sigma(2\chi \rightarrow 2X). \quad (3.40)$$

The parameters that describe the interactions and mass of the WIMP are all contained in the annihilation cross section.

Unlike other types of little Higgs models that have scalar dark matter candidates [25], in the model that we have described, the LPOP is the A_H , the little Higgs partner of the standard model hypercharge gauge boson, which we refer to as a heavy photon (see eq (2.13)). As shown in Section 2, the mass of this field to zeroth order in the expansion about the electroweak vacuum is directly related to the breaking scale of the $SU(5)$ global symmetry, f .

$$M_{A_H} = \frac{g' f}{\sqrt{5}}, \quad (3.41)$$

where g' is the standard model hypercharge gauge coupling. The partner of the photon is the LPOP due to the small gauge coupling, g' , as well as the factor of $\sqrt{5}$ that comes from the $SU(5)$ normalization of the $U(1)$ generators. The couplings of the A_H to the mass eigenstates are determined by the breaking scale f , and parameters in the Yukawa sector. However, the rate of annihilation to top quarks is small, therefore the annihilation coefficient is only weakly dependent on the new Yukawa couplings. The only remaining degree of freedom which governs the annihilation cross section is the mass of the Higgs. We calculate the annihilation cross section using COMPHEP [26], and based on the late time solution to (3.39), evaluate the relic density of the A_H dark matter. We use cosmological constraints on relic abundance of dark matter to find constraints on f . Of particular interest is the fact that relic abundance considerations put upper bounds on the breaking scale f , rather than just lower bounds. One could also use dark matter search constraints to find additional bounds on f , however we leave such work for future study.

3.1 Relic abundance calculation

The annihilation rate at a given center of mass velocity can be expanded in the non-relativistic limit as follows:

$$\sigma_{Av} = a + bv^2 + \dots \quad (3.42)$$

The coefficients a and b are determined by the couplings of the model being studied. If a is non zero, the dark matter candidate is referred to as an ‘s-annihilator’, and a ‘p-annihilator’ otherwise [27]. It is important here to distinguish the interactions of the little Higgs dark matter from SUSY dark matter. In supersymmetric theories, the WIMP is generally a p-annihilator, whereas in little Higgs theories, it will be an s-annihilator. This generally produces larger annihilation cross sections, and thus lower relic abundances.

In some models that contain dark matter, there are other particles which have a mass that is very close to that of the WIMP. In such cases, the relic abundance may be additionally depleted by processes that convert the WIMP to this nearly degenerate particle, which is then able to itself annihilate with other particles in the thermal bath. This process is called coannihilation. In the model that we consider, the A_H is always

much lighter than all of the other T-odd particles, as can be seen in the following formula:

$$\frac{m_{A_H}}{m_\phi} \approx \frac{g'v}{\sqrt{10}m_H} \approx .24 \quad \frac{m_{A_H}}{m_{Z_H}} \approx \frac{g'}{\sqrt{5}g} \approx .24, \quad (3.43)$$

where we have taken $m_H = 115$ GeV. Therefore coannihilation is not relevant in this model for the spectrum considered.

The techniques for solving the Boltzman equation for the population of the WIMP are well studied. One can numerically solve this equation, or one can use an approximate analytic result. This is generated by solving the early and late time behavior of the differential equation, and then matching in an intermediate region. We do not repeat this calculation, but simply quote the result. The relic abundance is given approximately by

$$\Omega_{\text{dm}} h^2 = \frac{1.07 \times 10^9 \text{GeV}^{-1} M}{g_*^{1/2} m_{\text{Pl}} \langle \sigma_{A_H} v \rangle T_F}, \quad (3.44)$$

where M is the mass of the WIMP, and T_F is the freezeout temperature, the temperature at which the Hubble term begins to dominate over the annihilation term. The term g_* is related to the number of relativistic degrees of freedom that exist at the time of freezeout. The freezeout temperature is dependent on the mass of the WIMP, though only weakly, and is determined through the solution of (3.39). For most WIMP dark matter, the freezeout temperature is roughly $M/20$. In this model, the number that we calculate is $T_F \approx M_{A_H}/22.5$ for most ranges of f and m_H .

If the cross section is too small, the WIMP does not annihilate enough before freeze out, and the relic density is larger than the experimental bounds allow. A somewhat less disturbing issue arises when the cross section is too large, and the relic density is too small to account for the total fraction of dark matter. In this situation, there must be another dark matter candidate to account for the remaining fraction, such as axions, which does not arise as part of the T-parity little Higgs mechanism. Current data coming from numerous astrophysical observables, most notably the WMAP sky survey [28], place the dark matter density (in units of the critical density) at

$$\Omega_{\text{DM}} h^2 = 0.111 \pm 0.006. \quad (3.45)$$

We calculate the annihilation cross section for the A_H in this littlest Higgs model with T-parity, and evaluate the resulting relic abundance as a function of the breaking scale f , and m_H . Annihilation to leptons and quarks occurs through either s-channel Higgs exchange, or T-odd fermion doublet exchange diagrams, both of which are suppressed due to smallness of the couplings. The exception to this is the annihilation to top quarks, which has a T-channel t_- singlet exchange diagram that is not suppressed. Additionally, there are effective Higgs-gluon-gluon and Higgs-photon-photon vertices coming from loop diagrams, but the annihilation cross section to these final states is negligible. The dominant contribution to the annihilation coefficient for most considered values of m_H and f arises from W^\pm production through Higgs exchange. The production of Z -bosons is also similarly

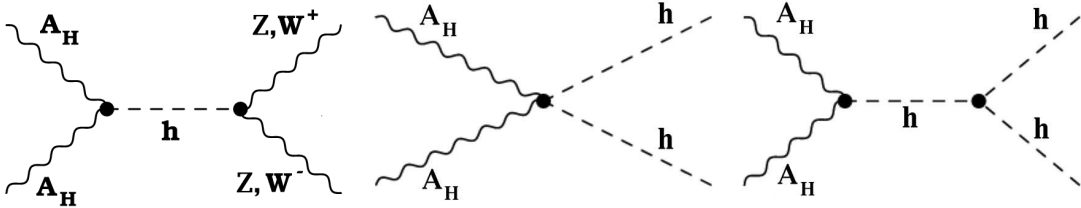


Figure 2: The A_H annihilates predominantly to SM gauge and Higgs bosons. These are the diagrams which give the largest contributions to the annihilation coefficient $\langle\sigma_{Av}\rangle$ for the ranges of f and m_H that we examine.

sizable, although approximately a factor of 4 smaller. The annihilation to Higgs pairs is also quite large when allowed by phase space, and dominates over annihilation to Z bosons, though the W^\pm channel still gives the largest contribution. The dominant diagrams from the primary channels are shown in Figure 2.

There are regions of parameter space in which the A_H is nearly equal to half the mass of an s-channel exchanged particle. In this scenario, there are s-channel poles in the annihilation cross section, and the diagrams which include such exchanges dominate the cross section. In this case, the annihilation rate is given by

$$\sigma_{Av} \approx \frac{\gamma^2 s}{(m^2 - s)^2 + m^2 \Gamma^2} \quad (3.46)$$

where Γ is the decay width of the exchanged particle, s is the center of mass energy squared, and γ^2 is a prefactor that is dependent on the couplings of the A_H to the exchanged particle. This is quite important in this model, due to the lightness of the A_H in comparison with the breaking scale, f . Many of the annihilation diagrams involve s-channel Higgs exchange, so when the Higgs has twice the mass of the heavy photon, the cross section will become quite large.

The resulting relic density is plotted in Figure 3.* It is conceivable that there is another relic in addition to the little Higgs dark matter, so we do not consider as ruled out regions where the A_H does not account for all of the dark matter. In the black regions, there is too much dark matter left over. This is generically a worse scenario, since it would overclose the universe, and we consider these regions to be ruled out if the heavy photon is stable. Interestingly, we find that small values of the Higgs mass are disfavored if the A_H is indeed the WIMP. Looking at Figure 3, one sees the importance of the s-channel Higgs exchange along the line $m_h = 2m_{A_H}$. Along this contour, the pole in the annihilation amplitude dominates the behavior of the annihilation cross section.

There are regions of parameter space where standard model particles are slightly heavier than the A_H , but there are still A_H particles on the high velocity end of the Boltzmann

*We are grateful to Maxim Perelstein and Andreas Birkedal for pointing out a factor of 4 error in our original calculation of the relic density.

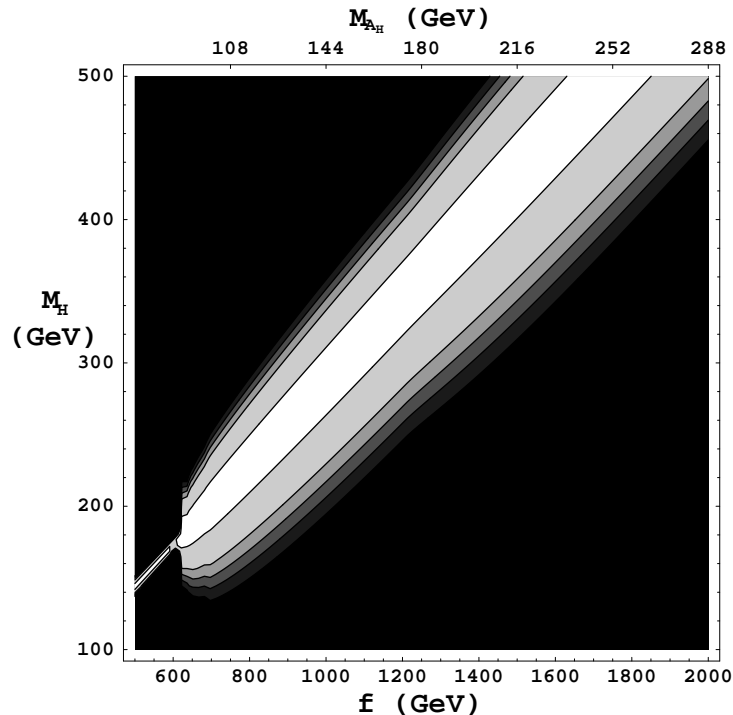


Figure 3: This plot depicts the variation of the relic density with respect to the Higgs mass and the symmetry breaking scale, f . In order from lightest to darkest regions, the A_H makes up (0 – 10%, 10 – 50%, 50 – 70%, 70 – 100%, 100%, > 100%) of the observed relic abundance of dark matter.

distribution, and which are thus energetic enough to be able to pair produce these slightly heavier particles, thus slightly increasing the thermally averaged cross section just below thresholds. In general, taking these corrections into account will smooth out the thermally averaged cross section as the mass of the A_H approaches such annihilation thresholds. It does strongly affect the overall fit, thus we neglect the threshold corrections in this paper.

The steep gradient of the relic density at $M_{A_H} \approx 80$ GeV is due to the threshold for annihilating to standard model W bosons. Below 80 GeV, the only available channels are to light fermions. These channels have very small associated amplitudes, as they require either the s-channel Higgs exchange which is suppressed by Yukawa couplings, or T -channel T -odd fermion doublet exchange. The T -channel fermion exchange diagrams are suppressed since the relevant couplings $A_H \Psi_{SM} \Psi_-$ are given by $g'/10 \approx .03$.

In the model that we have outlined, the strongest search constraints would come from nuclear recoil experiments and high energy solar and terrestrial neutrino searches. Other astrophysical searches, such as anomalous cosmic ray searches, would not likely be fruitful. This is because the dominant channels for such events require t-channel exchange of the heavy fermions, which, as mentioned above, involve small couplings $g'/10$, suppressing the relevant cross sections. In nuclear recoil experiments, however, because of the high

density of gluons in large nuclei, there is an enhancement of the nuclear scattering cross section from the effective higgs-gluon-gluon vertex. High energy neutrino searches rely on gravitational capture of the WIMP. From the same argument, the nuclear scattering cross section is sizeable, and serves to slow down WIMPs which encounter the sun or earth. The WIMPs are then captured gravitationally by the sun or earth. Subsequent annihilation of the A_H will potentially produce high energy neutrinos that reach detectors. We leave a full analysis of the dark matter search constraints for future research.

4 LHC Collider Phenomenology

The introduction of T-parity to the littlest Higgs adds new interesting features and avoids problems of other little Higgs models, but one must also check to see if there is any chance of detecting its consequences in future collider experiments. With T-parity one loses the ability to singly produce the new heavy vector bosons and scalars which is a major feature of how the original littlest Higgs could be detected [20, 21]. This is not entirely disheartening since the signal of the littlest Higgs will now become similar to that of the MSSM with a missing energy signal, which has been analyzed in great detail. In fact with the addition of T-parity type models it is even more difficult to determine what type of new physics is discovered at the LHC, since there are now more ways to fake a SUSY signal than there were before [29].

The littlest Higgs with T-parity has more varied collider signatures than just a missing energy signal which could fake SUSY. Not all of the new particles in the littlest Higgs with T-parity are T-odd. As in the original littlest Higgs model there is a T-even partner of the top quark which can be singly produced. The key difference in the littlest Higgs with T-parity compared to previous studies of the T-even partner of the top quark is the existence of the T-odd partner of the top quark, t'_- . The t'_- in fact will always be lighter than the t'_+ (see (2.33) and (2.34)). This will open up new decay channels for the t'_+ that did not exist in previous studies. These new decay channels can contribute a sizeable branching fraction to the t'_+ and thus new studies of the T-even sector of this model as well as the T-odd sector are required.

In this section we start the analysis of the collider phenomenology of the T-parity littlest Higgs. We choose sectors which capture the phenomenology of the scalar, gauge boson, and heavy fermion sectors that are common to all implementations of the T-parity littlest Higgs. We must emphasize here that a more general study including the additional T-odd fermions besides the t'_- should be undertaken, especially considering that the production cross sections involve strong rather than weak couplings. In Section 4.1 we will investigate the production mechanism for the T-odd particles in this model and the branching fractions for their decays. In Section 4.2 we will revisit the production and decay channels of the heavy T-even top that is now changed due to the presence of t'_- . We will then discuss in Section 4.3 the best search mechanisms as well as the associated backgrounds.

4.1 T-odd phenomenology

We will begin our study with the cross sections for pair producing T-odd particles. Implementing the model in COMPHEP [26] we compute production cross sections for the LHC. In the heavy gauge boson sector of the model there are no free parameters other than the scale f so the production cross sections at leading order are unambiguous. The cross section for pair producing heavy gauge bosons is plotted in Figure 4. For proton-proton scattering

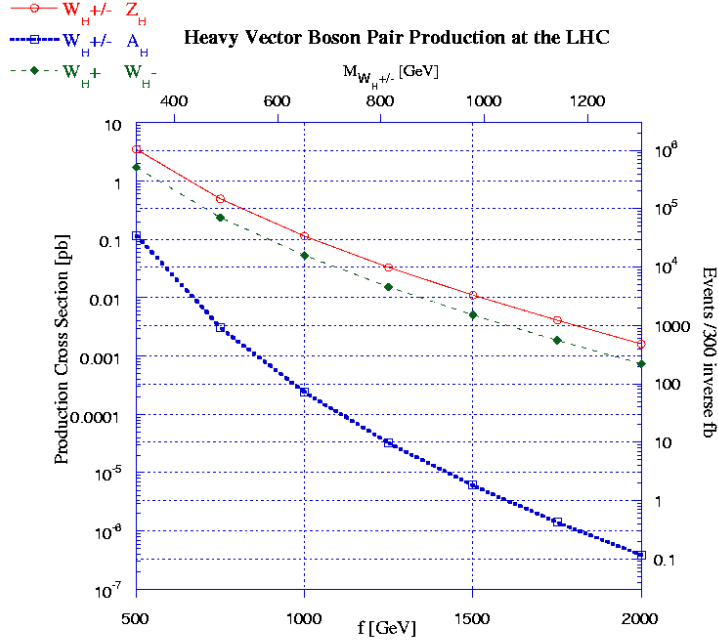


Figure 4: The cross section for the production of a pair of T-odd heavy vector bosons at the LHC is plotted as a function of the symmetry breaking scale f . The number of events for 300 fb^{-1} is plotted on the second y-axis. $M_{W_H^\pm}$ is plotted on the second x-axis. M_{Z_H} is degenerate in mass with $M_{W_H^\pm}$, and $M_{A_H} \sim .16f$.

at the LHC the dominant production channels are $W_H^\pm Z_H$ or $W_H^+ W_H^-$ pairs, while other channels such as $W_H^\pm A_H$ have lower total cross sections. For $W_H^\pm Z_H$ and $W_H^\pm A_H$ pairs, the production is from the exchange of a W^\pm ; however the $W_H^\pm A_H$ pairs interaction with the SM W^\pm is v/f suppressed. The $W_H^+ W_H^-$ pairs are produced through the exchange of a photon or Z . The decay channels of the heavy gauge bosons are simple since it turns out that they always decay directly to A_H , the lightest T-odd particle. The Z_H decays exclusively to $A_H h$ and the W_H^\pm decays entirely to $A_H W^\pm$.

The heavy triplet Φ is also T-odd and must be pair produced. The various components of the triplet ϕ^{++} , ϕ^+ , ϕ^0 , ϕ^- and their antiparticles all have the same mass at tree level. The mass of the Φ is related to the mass of the Higgs through the relation (2.15). In principle one should analyze all the different production channels for the components of

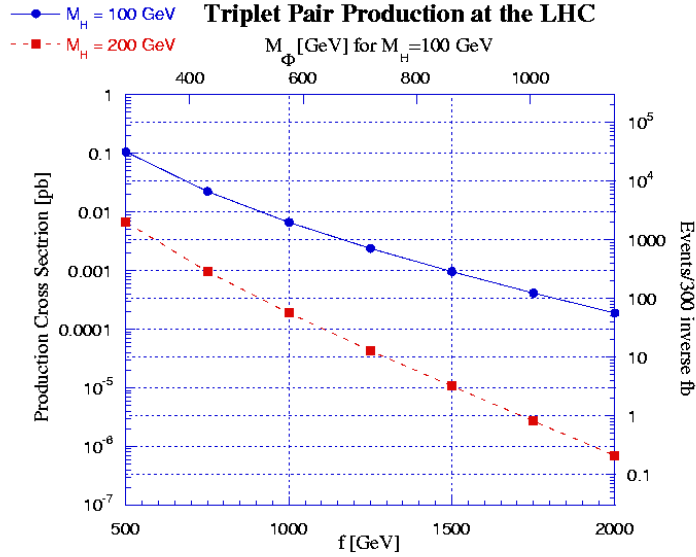


Figure 5: The cross section for the production of a pair of T-odd triplets at the LHC is plotted as a function of the symmetry breaking scale f . The cross section is plotted for $m_H = 100, 200$ GeV since the triplet mass, M_Φ , is determined by f and m_H . The number of events for 300 fb^{-1} is plotted on the second y-axis. M_Φ for a Higgs mass of 100 GeV is plotted on the second x-axis, for a Higgs mass of 200 GeV simply scale the second x-axis by a factor of 2.

Φ individually however to get an overall idea of the magnitude for pair producing Φ 's we sum the contribution for all channels and plot the cross section for the LHC in Figure 5. In Figure 5 since the mass of the Φ is determined by m_H and f we plot the production cross section as a function of f for two different values of m_H . The dominant channels for production of the triplet, in the naive scenario where all components of the triplet have the same mass, are for the charged components of Φ from W^\pm exchange. The decay of the components of the triplet are as simple as for the heavy gauge bosons since they each have only one decay channel. The charged components of the triplet decay in the following ways, $\phi^{++} \rightarrow W^+W_H^+$ and $\phi^+ \rightarrow AW_H^+$, with corresponding decay channels for the anti-particles. The pseudoscalar ϕ^P and scalar ϕ^0 decay through the processes $\phi^P \rightarrow HA_H$ and $\phi^0 \rightarrow ZA_H$.

The production process for the t'_- turns out to be very similar to pair producing t'_+ as in [21]. The reason why the production is the same as the t'_+ in this particular channel is that the production cross section is dominated by gluon exchange and is independent of all parameters except for $m_{t'_-}$. One should keep in mind that even though cross sections of t'_- and t'_+ have the same mass dependence, t'_- and t'_+ have in general different masses so they are produced at different rates. In Figure 6 we plot the cross section for producing the t'_- at the LHC as a function of its mass. The decay pattern of the t'_- is simple, the

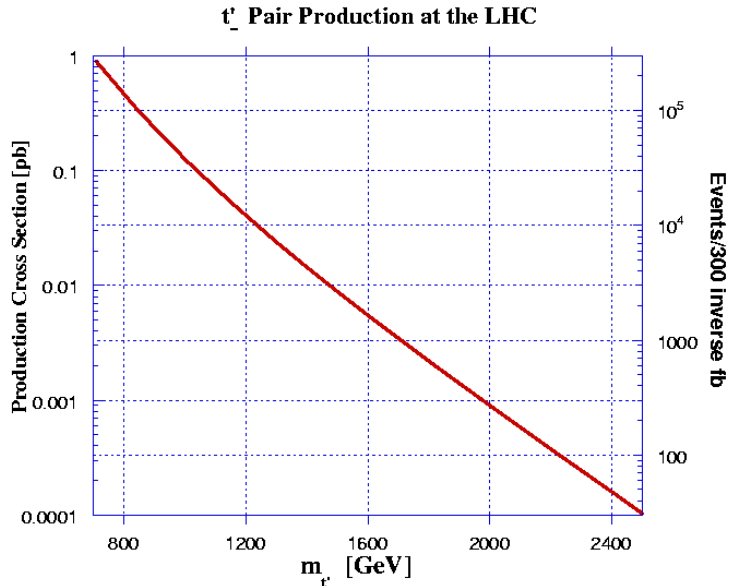


Figure 6: The cross section for the production of a pair of T-odd heavy quarks t'_- at the LHC is plotted as a function of $m_{t'_-}$. The number of events for 300 fb^{-1} is plotted on the second y-axis.

t'_- decays entirely to $A_H t$. The phenomenology of the t'_- merits further study since it will always be lighter than the t'_+ as well as having a large cross section for production. There may be other interesting channels for decay if one examines a different spectrum for the model. Since the cross section for producing the t'_- is so large it may be one of the more interesting ways to search for T-parity, however the backgrounds must be considered which will be done in Section 4.3.

4.2 T-even Top Quark

The main difference between R-parity SUSY models, the UED models with KK-parity that could fake a R-parity SUSY signal [29], and T-parity, is the existence of the t'_+ . The t'_+ is a generic feature of any little Higgs model and also any known model of T-parity. Comparing the interactions of t'_+ in the T-parity littlest Higgs to the original littlest Higgs model [4], one finds that the same interactions dominate the production cross section. The largest cross section for producing the t'_+ at the LHC is for singly producing a t'_+ and a jet, from T-channel W exchange. For low t'_+ mass a comparable cross section is for pair producing t'_+ however it drops rapidly with increasing mass. For a plot of the production cross section for the t'_+ we refer the reader to [21, 22] since the results are the same for this model.

Even though the production cross sections for the t'_+ are the same in T-parity models as for non T-parity models at the LHC, there is an important difference in the phenomenology

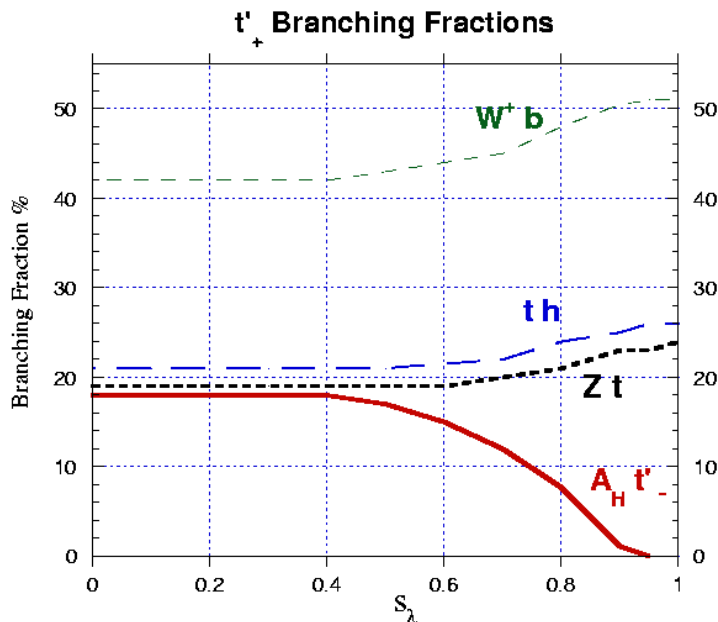


Figure 7: We plot the branching fractions for t'_+ decay as a function of s_λ , which parameterizes the ratio of masses of the t'_+ and t'_- . This plot was generated for $f = 1$ TeV

of the t'_+ . The existence of the t'_- which is always required to be less massive than the t'_+ from (2.34) and (2.33) opens a new decay channel for the t'_+ . In Figure 7 we plot the branching fractions of the t'_+ as a function of $s_\lambda = \frac{m_{t'_-}}{m_{t'_+}}$. The branching fraction is essentially independent of f . As one can see from Figure 7, for most of parameter space the t'_+ has a sizeable invisible width from decay to $t'_- A_H$. In reality though to solve the little hierarchy problem one is only interested in the region around $s_\lambda = \frac{1}{\sqrt{2}}$ where $m_{t'_+} = \sqrt{2}f$. For either direction in s_λ , $m_{t'_+}$ increases which causes a fine tuning of the Higgs mass if $m_{t'_+}$ is larger than ~ 2 TeV. The existence of this new sizeable invisible width of the t'_+ does not let one apply the analysis of [22] for the t'_+ in T-parity models. In [22] it was hoped that one could test the little Higgs mechanism for the t'_+ by measuring the couplings of the t'_+ and f independently, since they must satisfy a particular relationship to cancel the one-loop quadratically divergent contributions to the Higgs mass from the top quark. In T-parity type models one first has a difficulty with measuring f because one cannot obtain f from the gauge boson sector as in [20]. In addition, the new sizeable partial width of the t'_+ , which is hard to determine, makes measuring the couplings of the heavy partner of the top quark at the LHC virtually impossible.

4.3 Backgrounds and Best Signals

In the previous parts of this section we have studied the tree-level production cross sections for the LHC and found a large number of events for certain processes. However when dealing with a hadron collider the background tends to be ubiquitous so the question remains, for the interesting processes can one distinguish signal from background? To begin analyzing this question we compute the tree level production cross sections for irreducible backgrounds at the level of SM gauge and Higgs bosons. This analysis is not at the level of a physical background in a detector, however a signal must pass this simple test before taking into account the full background. For those processes where we find the signal is much higher than the simple backgrounds we analyze, we comment on the full backgrounds. A full analysis of the backgrounds is required but we leave this for future work.

We will start by looking at the backgrounds for the pair production of heavy gauge bosons. From Section 4.1 the strongest production mechanisms for the heavy gauge bosons are in the channels $W_H^\pm Z_H$ and $W_H^+ W_H^-$. Since the heavy gauge bosons have only one decay channel each, the final state (after the heavy particles have decayed) will be

$$\begin{aligned} pp &\rightarrow W_H^\pm Z_H \rightarrow W^\pm h A_H A_H \\ pp &\rightarrow W_H^+ W_H^- \rightarrow W^+ W^- A_H A_H. \end{aligned} \quad (4.1)$$

The signature in the detector will then be missing energy from the A_H along with the decay products of the SM particles. For the simple irreducible background we are interested in, we look for SM processes which have the same SM particles (at the level of gauge and Higgs bosons) as (4.1) along with missing energy in the final state. The dominant process of this type in the SM are to include a Z in the final state in place of the A_H 's, which then decays to neutrinos. Thus our estimate will be to compute the production cross section at the LHC for the final states of (4.1) replacing the A_H 's with a single Z and then multiplying by the branching fraction for the invisible decay of the Z .

For $W_H^+ W_H^-$ production one has to compete with a background of triple gauge boson production $W^+ W^- Z$ which has a production cross section, taking into account the Z branching fraction, of $\sim 10^{-2}$ pb. Comparing this background rate to the signal found in Fig. 4, we find that the signal is larger than the background for small values of f . To determine whether the signal is actually observable, since the signal passes this test for a certain range of f one must also consider the other processes which have the same final state in the detector (not just at the level of gauge and Higgs bosons). In the detector the possibilities for this channel are

$$pp \rightarrow W_H^+ W_H^- \rightarrow 4 \text{ jets} + \text{MET}, \quad (4.2)$$

$$\rightarrow 2 \text{ jets} + l + \text{MET}, \quad (4.3)$$

$$\rightarrow 2l + \text{MET}. \quad (4.4)$$

Ignoring the 4 jets + MET channel for its inherent difficulties, unfortunately this type of

signal ((4.3) and (4.4)) in a detector has a background from

$$pp \rightarrow W^+ W^- \quad (4.5)$$

which has a production cross section of $\mathcal{O}(\text{pb})$ at the LHC. This background is significantly larger than the signal and makes discovery in the $W_H^+ W_H^-$ channel very difficult. Since the MET from the signal will be very energetic with the application of cuts perhaps some signal can be distinguished from background but it would be very difficult.

For the $W_H^\pm Z_H$ production channel our simple irreducible background estimate comes from $W^\pm h Z$ production. The total production cross section for this background, taking into account the branching fraction of $Z \rightarrow$ invisible, is $\sim 10^{-3}$ pb. When comparing this background rate to the signal using Fig. 4 we find that for all values of f the signal is larger than the background and for $f \sim 1$ TeV the signal is almost two orders of magnitude larger. This is relatively easy to understand since producing a Higgs with two gauge bosons is difficult in the SM. However, we must estimate a more realistic background for this process as we did for the $W_H^+ W_H^-$ channel, before deciding whether this is a promising channel. For low Higgs mass the Higgs will decay predominantly into b jets, so to avoid looking for a 4 jet plus MET signal, we consider the W decaying into a lepton plus MET. Therefore the backgrounds can come from

$$pp \rightarrow h W^\pm \rightarrow 2 b \text{ jets} + l + \text{MET}, \quad (4.6)$$

$$\rightarrow Z W^\pm \rightarrow 2 b \text{ jets} + l + \text{MET}, \quad (4.7)$$

$$(4.8)$$

which will have a rate comparable to the signal we are interested in, making discovery in this channel also unlikely. However further study of this channel would be interesting, since it has the highest rate of production of the heavy gauge bosons.

The production of the triplet Φ is even less promising than the heavy gauge bosons since the production cross section is lower, Fig. 5, and the backgrounds are more complicated. In general the signal for pair producing components of Φ will be the SM decay products of multiple gauge bosons along with missing energy. The most promising component of the triplet is the pseudoscalar ϕ^P which decays to $A_H h$, since the Higgs is a more unique signal than SM gauge bosons. The two ways to produce a ϕ^P come from

$$\begin{aligned} pp &\rightarrow \phi^\pm \phi^P \rightarrow W^\pm A h A_H A_H \\ pp &\rightarrow \phi^0 \phi^P \rightarrow h Z A_H A_H. \end{aligned} \quad (4.9)$$

The cross section for the production channel $\phi^0 \phi^P$ is of the order 10^{-4} pb, for a Higgs mass of 115 GeV and $f = 1$ TeV, while the simple irreducible background, which was estimated as before by replacing the A_H with a Z decaying invisibly, is of the same order. Since the signal for $\phi^0 \phi^P$ is not larger than even the naive background we don't consider the full background for this channel. A slightly more promising channel is the $\phi^\pm \phi^P$ which also has a cross section for production of the order 10^{-4} pb for a Higgs mass of 115 GeV

and $f = 1$ TeV. The simple irreducible background in this case would be a final state $W^\pm AhZ$ with the Z decaying invisibly. This background at tree level is of the order 10^{-6} pb which seems promising. However with so few events from the signal, any enhancement of the background beyond this naive estimation could prove troublesome. The signal in the detector for this process, assuming the Higgs decays to b jets and the W to leptons, is

$$pp \rightarrow 2 b \text{ jets} + l + A + \text{MET}. \quad (4.10)$$

The physical background for this signal could come from W, A, h production. The production rate for this background is comparable to the signal so it does not appear promising. However, the photon would be very energetic coming from the decay of ϕ^\pm so perhaps a cut could be made to reduce the background.

The detection of the t'_+ in the littlest Higgs model without T-parity has been extensively investigated for the LHC in a study for the ATLAS detector [30]. The only difference for the t'_+ when including T-parity is the sizeable new contribution to its width from the t'_- as discussed in Section 4.2. The t'_- is one of the most interesting new parts of the T-parity littlest Higgs since it doesn't exist in non T-parity little Higgs models, and it is required to be lighter than the t'_+ , which in turn is required to be approximately at a TeV to avoid fine tuning. Even though the t'_- is perhaps the most interesting new particle from the model building perspective, it will be difficult to discern at the LHC. The t'_- decay pattern gives a background at the LHC of $t\bar{t} + \text{MET}$. The production rate for $t\bar{t} + \text{MET}$ at the LHC is large, making it difficult to find this signal above background.

5 Conclusions

In this paper we have given a review of the implementation of T-parity in the littlest Higgs model and begun the study of its phenomenology. There are several implementations of T-parity in the littlest Higgs as discussed in Section 2.2. We studied the phenomenology of a particular implementation that has the same basic features of any implementation of littlest Higgs with T-parity. In studying the dark matter candidate of the littlest Higgs with T-parity (if T-parity is conserved), which is the heavy photon A_H , we find that it can account for the observed relic density of dark matter in the universe. Assuming that the A_H is stable, we find bounds on the symmetry breaking scale f as a function of m_H , and that lower values of m_H are disfavored. We have begun the study of the collider phenomenology of the littlest Higgs with T-parity. We find that the generic signal for this model will be a missing energy signal similar to that of SUSY. The littlest Higgs model with T-parity offers a distinct alternative to SUSY for stabilizing the electroweak scale, and could be thought of as a “bosonic” supersymmetry since it could fake a SUSY signal at the LHC. We find that since one must pair produce T-odd particles the signal will be very difficult to distinguish from the background, which is very different than the littlest Higgs model without T-parity [20, 21]. The T-parity littlest Higgs also has a heavy T-even top quark partner t'_+ which distinguishes itself from a supersymmetric model or one designed to fake

a supersymmetric signal. The production mechanisms of the t'_+ turn out to be identical to the lightest Higgs without T-parity, however we find that in introducing T-parity one is required to introduce a T-odd t'_- with a mass required to be lighter than that of the t'_+ . The t'_- changes the phenomenology of the t'_+ , and thus existing studies of the t'_+ are not directly applicable for determining its properties.

There are many avenues for future research on the lightest Higgs with T-parity and we list some of the most important in our opinion. We have found bounds on the scale f from the analysis of the dark matter candidate (under the assumption that T-parity is conserved), however, a full analysis of EW precision constraints including loop contributions needs to be done to find complementary constraints. The discovery channels that we have discussed need to be further investigated beyond our simple treatment of the background to see if this model can really be distinguished or not from the ubiquitous background of the LHC. One might also investigate the T-odd fermion spectrum, which is quite interesting from the standpoint of phenomenology. We analyzed only the gauge, scalar, and top sectors, however in principle all the new fermions could be within reach of the LHC making the parameter space much larger and give other opportunities for discovery. A study of how to distinguish the lightest Higgs with T-parity from the MSSM (or other models designed to fake SUSY) at the LHC is also of paramount interest. The t'_+ would be an obvious distinguishing characteristic of T-parity however it could be out of the discovery reach of the LHC. Although the existence of T-parity greatly complicates deciphering the data of the LHC, it provides an interesting solution to the little hierarchy problem that deserves further study.

Acknowledgments

We would like to thank Maxim Perelstein for useful discussions as well as reading the manuscript and making helpful comments. We would like to thank Ian Low for clarification of some aspects of the T-parity models. We would also like to thank Csaba Csáki and Konstantin Matchev for reading the manuscript and making helpful comments. J.H. and P.M would like to thank the University of Colorado at Boulder TASI program, and P.M would like to thank the T-8 group at Los Alamos National Lab for hospitality and support while this work was in progress. The research of J.H. and P.M. is supported in part by the NSF under grant PHY-0355005.

A Four Fermion Operators

The four fermion operators that ruled out the models of [18] are absent in this model, since the standard model fermions transform linearly. However, there are still finite diagrams which are potentially dangerous, and must be checked. In the model that we discuss, the

types of diagrams are shown in Figure 8. By NDA, these diagrams give effective four-fermion contact terms which are approximately given by:

$$\frac{g^4 \kappa^2}{16\pi^2 \lambda^2 x^2 f^2}, \quad \frac{g^4}{16\pi^2} \left(\frac{1}{\lambda f} \right)^2 \quad \text{and} \quad \frac{\kappa^4}{16\pi^2} \left(\frac{1}{\lambda f} \right)^2, \quad (\text{A.1})$$

respectively. The parameter x refers to the ratio of the pion mass to the breaking scale, f . We have taken x to be larger than g . In order to avoid bounds on such contact terms, these must be less than $1/(5 - 10\text{TeV})^2$.

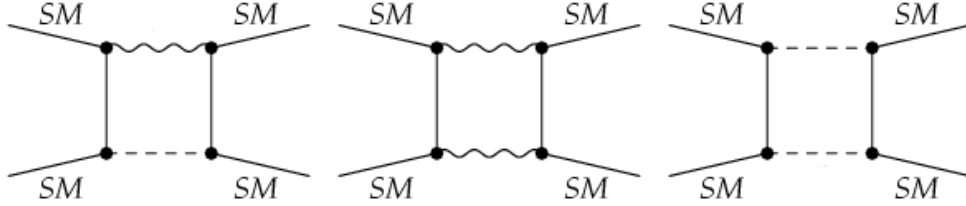


Figure 8: These diagrams, where the particles running in the loop are all odd under T-parity, lead to potentially dangerous four-fermion operators. In these diagrams, the scalar propagators represent pion exchange, and the gauge boson propagators refer to exchange of any of the A_H , Z_H , or W_H^\pm . The fermion lines in the loops represent exchange of the heavy T-odd fermions.

One might expect that these can be easily suppressed by taking λ to be large, however a more careful analysis is required. The interactions involving the coupling κ originate from the heavy fermion Yukawas

$$\kappa f (\bar{\Psi}_2 \xi \Psi' + \bar{\Psi}_1 \Sigma_0 \Omega \xi^\dagger \Omega \Psi'). \quad (\text{A.2})$$

where the fermion multiplets are given by

$$\Psi_1 = \begin{pmatrix} \psi_1 \\ 0 \\ 0 \end{pmatrix} \quad \Psi_2 = \begin{pmatrix} 0 \\ 0 \\ \psi_2 \end{pmatrix} \quad \Psi' = \begin{pmatrix} \tilde{\psi}' \\ \chi' \\ \psi' \end{pmatrix}. \quad (\text{A.3})$$

It is from this term that the diagrams with Goldstone boson exchange in the loop emerge. However, this term is also generating a mass term $\sqrt{2}\kappa$ for the Dirac pair $(\psi_2 + \psi_1, \psi')$. This could potentially give a fixed relation between κ and λ that would force the parameter κ to be relatively small, prohibiting a decoupling limit. For example, if the mass of the heavy fermion is $\sqrt{2}\kappa$, then the contact operator would be

$$\frac{\kappa^4}{32\pi^2} \left(\frac{1}{\kappa f} \right)^2 = \frac{\kappa^2}{32\pi^2 f^2}. \quad (\text{A.4})$$

In this case, we would require $\kappa < 0.5 - 1.5$ for $f = 1$ TeV.

Most of the interactions in (A.2), however, do not lead to amplitudes where we have such a relation, and many of the fermion masses can be made quite heavy. In particular, it is only the right handed doublet, ψ' which must be kept close to the breaking scale f . The four-fermion operator that involves ψ' exchanges the Goldstones which are eaten by the heavy vector fields W_H and Z_H , and these operators can not be suppressed since it is ψ' which gets its mass from the Yukawa interaction in Eq. (A.2).^{*} All of the vertices appearing in Figure 8 that involve the triplet, Φ couple the standard model fermion to the doublet $\tilde{\psi}'$, rather than ψ' . The parameters λ that appear in the four fermion diagrams above are then independent of κ . Simply taking $\lambda > \kappa^2$ suppresses the dangerous amplitudes. We note, though, that we do not take λ to the strong coupling limit. First, this would be dangerous for potential quartic divergences in the Higgs mass [18]. Second, we are attempting to avoid taking any parameters in the theory into a non-perturbative regime.

We have shown here that we can in fact raise the masses of the many of the additional fermions above the minimal little Higgs spectrum. In example, for an f of 1 TeV, the masses of most T-odd fermions are all at 5 TeV, safe enough to neglect in collider and dark matter phenomenology, yet light enough to avoid theoretical issues involving large contributions to the Higgs mass through two loop quartically divergent diagrams. The couplings required to raise the masses sufficiently are still within the perturbative regime, so we have not resorted to a strong coupling limit. With the resulting TeV scale spectrum, we compute the phenomenology of a littlest Higgs with T-parity which is similar to the low energy limit of the other models which incorporate this discrete symmetry. We leave an analysis of the lighter T-odd partners of the standard model doublets for future research.

B Feynman Rules for the Littlest Higgs with T-parity

In this appendix we will provide a list of Feynman rules specific to the T-parity littlest Higgs as a reference to facilitate further study of the model. As discussed in Section 2 implementing T-parity in the littlest Higgs for the gauge and scalar sectors does not require a drastic change to the structure of the original littlest Higgs. The effect in the gauge sector is to set the gauge couplings, g_j , in the original littlest Higgs to be $g_1 = g_2 = \sqrt{2}g$, and likewise for the g' couplings. In the scalar sector the effect is essentially to forbid a VEV for the triplet Φ by forbidding the T-odd coupling $H\Phi H$. With this in mind a great many of the Feynman rules can be obtained from [21] which listed all the Feynman rules for the littlest Higgs. We will give a guide to how to obtain the T-parity Feynman rules from the Feynman rules in [21]. We then will list the additional Feynman rules specific to the T-parity littlest Higgs.

If one uses Tables I-VIII in [21] for the Feynman rules in the scalar and gauge sectors, it is necessary to apply the following rules for the parameters in [21] to obtain the correct

^{*}We thank Thomas Gregoire for pointing out that this is the relevant four fermion diagram that prevents decoupling the T-odd fermion spectrum completely.

Particles	Vertices	Particles	Vertices
$W_H^{-\mu}W^{+\nu}\phi^P$	$\frac{g^2}{3\sqrt{2}}\frac{v^2}{f}g_{\mu\nu}$	$Z^\mu Z_H^\nu\phi^0$	$-i\frac{g^2}{2\sqrt{2}c_w}\frac{v^2}{f}g_{\mu\nu}$
$A_H^\mu Z^\nu\phi^0$	$i\frac{g^2}{2\sqrt{2}s_w}\frac{v^2}{f}g_{\mu\nu}$	$W_H^{+\mu}Z^\nu\phi^-$	$i\frac{g^2}{12c_w}(1+2s_w^2)\frac{v^2}{f}g_{\mu\nu}$
$W_H^{+\mu}A^\nu\phi^-$	$-i\frac{eg}{6}\frac{v^2}{f}g_{\mu\nu}$	$W^{+\mu}A_H^\nu\phi^-$	$-i\frac{gg'}{4}\frac{v^2}{f}g_{\mu\nu}$
$Z_H^\mu W^{+\nu}\phi^-$	$i\frac{5g^2}{12}\frac{v^2}{f}g_{\mu\nu}$	$W^{-\mu}W_H^{-\nu}\phi^{++}$	$-i\frac{g^2}{2}\frac{v^2}{f}g_{\mu\nu}$
$W_H^{-\mu}W^{+\nu}\phi^Ph$	$\frac{\sqrt{2}g^2}{3}\frac{v}{f}g_{\mu\nu}$	$Z^\mu Z_H^\nu\phi^0h$	$-i\frac{g^2}{\sqrt{2}c_w}\frac{v}{f}g_{\mu\nu}$
$A_H^\mu Z^\nu\phi^0h$	$i\frac{g^2}{\sqrt{2}s_w}\frac{v}{f}g_{\mu\nu}$	$W_H^{+\mu}Z^\nu\phi^-h$	$i\frac{g^2}{6c_w}(1+2s_w^2)\frac{v}{f}g_{\mu\nu}$
$W_H^{+\mu}A^\nu\phi^-h$	$-i\frac{eg}{3}\frac{v}{f}g_{\mu\nu}$	$W^{+\mu}A_H^\nu\phi^-h$	$-i\frac{gg'}{2}\frac{v}{f}g_{\mu\nu}$
$Z_H^\mu W^{+\nu}\phi^-h$	$i\frac{5g^2}{6}\frac{v}{f}g_{\mu\nu}$	$W^{+\mu}W_H^{+\nu}\phi^{--}h$	$-ig^2\frac{v}{f}g_{\mu\nu}$
$Z_H^\mu Z_H^\nu\phi^0\phi^0$	$i\frac{g^2}{12}\frac{v^2}{f^2}g_{\mu\nu}$	$A_H^\mu A_H^\nu\phi^0\phi^0$	$i\frac{g^2}{12}\frac{v^2}{f^2}g_{\mu\nu}$
$Z_H^\mu A_H^\nu\phi^0\phi^0$	$-i\frac{gg'}{12}\frac{v^2}{f^2}g_{\mu\nu}$	$W_H^{+\mu}A_H^\nu\phi^0\phi^-$	$i\frac{x_h g^2}{15\sqrt{2}c_w^2}(10-9s_w^2)\frac{v^2}{f^2}g_{\mu\nu}$
$W_H^{+\mu}W_H^{-\nu}\phi^+\phi^-$	$i\frac{g^2}{24}\frac{v^2}{f^2}g_{\mu\nu}$	$A_H^\mu A_H^\nu\phi^+\phi^-$	$i\frac{g^2}{24}\frac{v^2}{f^2}g_{\mu\nu}$
$Z_H^\mu A_H^\nu\phi^+\phi^-$	$i\frac{x_h g^2}{30c_w^2}(25-18s_w^2)\frac{v^2}{f^2}g_{\mu\nu}$	$W_H^{+\mu}A_H^\nu\phi^+\phi^{--}$	$-i\frac{x_h g^2}{15c_w^2}(5-3s_w^2)\frac{v^2}{f^2}g_{\mu\nu}$
$Z_H^\mu Z_H^\nu\phi^P\phi^P$	$i\frac{g^2}{12}\frac{v^2}{f^2}g_{\mu\nu}$	$A_H^\mu A_H^\nu\phi^P\phi^P$	$i\frac{g^2}{12}\frac{v^2}{f^2}g_{\mu\nu}$
$Z_H^\mu A_H^\nu\phi^P\phi^P$	$-i\frac{gg'}{12}\frac{v^2}{f^2}g_{\mu\nu}$	$W_H^{+\mu}A_H^\nu\phi^P\phi^-$	$-\frac{x_h g^2}{15\sqrt{2}c_w^2}(10-9s_w^2)\frac{v^2}{f^2}g_{\mu\nu}$
$W_H^{+\mu}h\phi^-$	$i\frac{g}{6}\frac{v}{f}(p_1-2p_2)_\mu$	$A_H^\mu h\phi^P$	$\frac{g'}{3\sqrt{2}}\frac{v}{f}(p_1-2p_2)_\mu$
$Z_H^\mu h\phi^P$	$-\frac{g}{3\sqrt{2}}\frac{v}{f}(p_1-2p_2)_\mu$		

Table 2: Feynman rules for the gauge and scalar sector of the T-parity littlest Higgs that can not be determined from the appendix of [21]. The momenta are all defined as outgoing and for the gauge-scalar-scalar vertices, the momenta refer to the first and second scalar respectively.

vertices for the T-parity littlest Higgs model:

$$c = s = c' = s' = \frac{1}{\sqrt{2}}, \quad (\text{B.5})$$

$$s_0 = s_P = s_+ = 0, \quad (\text{B.6})$$

$$c_0 = c_P = c_+ = 1. \quad (\text{B.7})$$

However when using (B.5) with the tables referred to in [21] certain T-even interactions will naively be set to 0 since T-parity will cause certain interactions to start at a higher order in a v/f expansion than taken into account. These interactions that can not be found in [21] need to be included for studying certain phenomenological processes. As an example certain components of the Φ would be unnaturally long lived since most decay channels are missing if one does not include the higher order interactions. In Table 2 we list the Feynman rules for T-parity even interactions that are zero in the order considered by [21]. The parameters s_w and c_w refer to the sine and cosine of the weak mixing angle θ_w , while

$$x_h = \frac{5}{4} \frac{gg'}{5g^2 - g'^2}. \quad (\text{B.8})$$

The fermion sector of the littlest Higgs with T-parity is radically different than the original littlest Higgs model, therefore the Feynman rules of [21] do not apply. The SM fermions of the first two generation of quarks and all three generations of leptons have their usual SM couplings. However, in the third generation the new Yukawa interactions required to cancel the quadratic divergences of the top quark will shift some SM couplings at $\mathcal{O}(v^2/f^2)$. The t'_+ and t'_- couplings are also new in the T-parity littlest Higgs so we will include all these Feynman rules in Table 3 and Table 4.

Particles	Vertices	Particles	Vertices
$\bar{t}th$	$-i\frac{m_t}{v}$	$\bar{t}thh$	$i\frac{m_t(1+s_\lambda^2)}{f^2}$
$\bar{t}t\phi^0\phi^0$	$i\frac{2m_t}{3f^2}(-2+3s_\lambda^2)$	$\bar{t}t\phi^P\phi^P$	$i\frac{2m_t}{3f^2}(-2+3s_\lambda^2)$
$\bar{t}t\phi^-\phi^+$	$i\frac{2m_t}{3f^2}(-1+3s_\lambda^2)$	$\bar{t}t\phi^{--}\phi^{++}$	$i\frac{2m_t s_\lambda^2}{f^2}$
$t'_+t'_+h$	$i\frac{m_t c_\lambda s_\lambda}{f}$	$t'_+t'_+hh$	$i\frac{m_t c_\lambda}{v f s_\lambda}$
$t'_+t'_+\phi^0\phi^0$	$i\frac{2m_t c_\lambda}{v f s_\lambda}$	$t'_+t'_+\phi^P\phi^P$	$i\frac{2m_t c_\lambda}{v f s_\lambda}$
$t'_+t'_+\phi^-\phi^+$	$i\frac{2m_t c_\lambda}{v f s_\lambda}$	$t'_+t'_+\phi^{--}\phi^{++}$	$i\frac{2m_t c_\lambda}{v f s_\lambda}$
\bar{t}'_+th	$-im_t\left(\frac{s_\lambda^2}{f}P_R - \frac{c_\lambda}{s_\lambda v}P_L\right)$	\bar{t}'_+thh	$-i\frac{m_t}{f}\left(\frac{1}{v}P_R + \frac{(1+s_\lambda^2)c_\lambda}{s_\lambda f}P_L\right)$
$\bar{t}'_+t\phi^0\phi^0$	$-2i\frac{m_t}{f}\left(\frac{1}{v}P_R - \frac{(2-3s_\lambda^2)c_\lambda}{3s_\lambda f}P_L\right)$	$\bar{t}'_+t\phi^P\phi^P$	$-2i\frac{m_t}{f}\left(\frac{1}{v}P_R - \frac{(2-3s_\lambda^2)c_\lambda}{3s_\lambda f}P_L\right)$
$\bar{t}'_+t\phi^-\phi^+$	$-2i\frac{m_t}{f}\left(\frac{1}{v}P_R - \frac{(1-3s_\lambda^2)c_\lambda}{3s_\lambda f}P_L\right)$	$\bar{t}'_+t\phi^{--}\phi^{++}$	$-2i\frac{m_t}{f}\left(\frac{1}{v}P_R + \frac{c_\lambda s_\lambda}{f}P_L\right)$
$\bar{t}'_-t'_+\phi^P$	$\sqrt{2}m_t\frac{c_\lambda v}{3f^2 s_\lambda}P_R$	$\bar{t}'_-t'_+\phi^P h$	$2\sqrt{2}m_t\frac{c_\lambda}{3f^2 s_\lambda}P_R$
$\bar{t}'_-t\phi^P$	$-\sqrt{2}m_t\frac{v}{3f^2}P_R$	$\bar{t}'_-t\phi^P h$	$-\sqrt{2}m_t\frac{2}{3f^2}P_R$
$\bar{b}t\phi^0\phi^-$	$im_t\frac{2}{3f^2}P_R$	$\bar{b}t\phi^P\phi^-$	$-m_t\frac{2}{3f^2}P_R$
$\bar{b}t\phi^+\phi^{--}$	$im_t\frac{2\sqrt{2}}{3f^2}P_R$	$\bar{b}t'_+\phi^0\phi^-$	$-im_t\frac{2c_\lambda}{3s_\lambda f^2}P_R$
$\bar{b}t'_+\phi^P\phi^-$	$m_t\frac{2c_\lambda}{3s_\lambda f^2}P_R$	$\bar{b}t'_+\phi^+\phi^{--}$	$-im_t\frac{2\sqrt{2}c_\lambda}{3s_\lambda f^2}P_R$

Table 3: Feynman rules for the third generation quarks-scalars which are shifted from the SM vertices, and interactions of the t'_+ and t'_- quarks with scalars. $P_L = \frac{1-\gamma^5}{2}$ and $P_R = \frac{1+\gamma^5}{2}$ are the usual LH and RH projectors.

The phenomenology of the littlest Higgs with T-parity could be markedly changed by the inclusion of the additional fermions around the TeV scale. There exist interactions of heavy fermions with SM particles that come from re-expressing the kinetic terms in mass eigenstates, and are generally of the form

$$c\bar{\psi}_{SM}\bar{\sigma}_\mu V_H^\mu\psi_H, \quad (\text{B.9})$$

as shown in Section 2. These interactions potentially can be flavor changing depending on the implementation of the heavy mirror fermion Yukawa term (2.20). There are also

Particles	Vertices	Particles	Vertices
$t'_- t'_- G^\mu$	$ig_s \gamma_\mu$	$t'_+ t'_+ G^\mu$	$ig_s \gamma_\mu$
$A_H^\mu \bar{t}'_+ t'_-$	$\frac{2ig'}{5} \gamma_\mu (P_L + s_\lambda P_R)$	$A_H^\mu \bar{t}'_- t$	$\frac{2ig'}{5} c_\lambda \gamma_\mu (c_\lambda \frac{v}{f} P_L + P_R)$
$Z_H^\mu \bar{t}'_- t$	$\frac{2}{5} ix_h g' c_\lambda \frac{v^2}{f^2} \gamma_\mu P_R$	$Z_H^\mu \bar{t}'_- t'_+$	$\frac{2}{5} ix_h g' \frac{v^2}{f^2} \gamma_\mu (P_L + s_\lambda P_R)$
$A^\mu \bar{t}'_+ t'_+$	$\frac{2}{3} ie \gamma_\mu$	$A^\mu \bar{t}'_- t'_-$	$\frac{2}{3} ie \gamma_\mu$
$Z^\mu \bar{t} t$	$\frac{ig}{c_w} \gamma_\mu \left(\left(\frac{1}{2} - 2/3 s_w^2 - \frac{1}{2} \frac{v^2}{f^2} c_\lambda^4 \right) P_L - \frac{2}{3} s_w^2 P_R \right)$	$Z^\mu \bar{t}'_+ t'_+$	$-\frac{2}{3} \frac{ig}{c_w} s_w^2 \gamma_\mu + \frac{1}{2} \frac{ig}{c_w} \frac{v^2}{f^2} c_\lambda^4 P_L$
$Z^\mu \bar{t}'_- t'_-$	$-\frac{2}{3} \frac{ig}{c_w} s_w^2 \gamma_\mu$	$Z^\mu \bar{t}'_+ t$	$-\frac{1}{2} \frac{ig}{c_w} \frac{v}{f} c_\lambda^2 \gamma_\mu P_L$
$W^{+\mu} \bar{t} b$	$\frac{V_{tb}}{\sqrt{2}} ig \gamma_\mu \left(1 - \frac{c_\lambda^4}{2} \frac{v^2}{f^2} \right) P_L$	$W^{+\mu} \bar{t}'_+ b$	$-\frac{ig}{\sqrt{2}} V_{tb} \frac{v}{f} c_\lambda^2 \gamma_\mu P_L$

Table 4: Feynman rules for the third generation quarks which are shifted from the SM vertices, and interactions of the t'_+ and t'_- quarks. $P_L = \frac{1-\gamma^5}{2}$ and $P_R = \frac{1+\gamma^5}{2}$ are the usual LH and RH projectors.

interactions similar to (B.9) which involve heavy scalars instead of heavy vector bosons which come from (2.20). Finally there are interactions of heavy fermions with SM gauge bosons coming from (2.24) and (2.26). We do not include the Feynman rules for these interactions, since they were not necessary for the sectors studied in this paper, and they are dependent upon the implementation (in terms of flavor) of the mirror fermion mass terms. For the reader interested in investigating the fermion sector of the model in more detail, one must choose an implementation of flavor for the heavy mirror fermion Yukawa's (2.20) and work out the interactions.

References

- [1] N. Arkani-Hamed, A. G. Cohen and H. Georgi, Phys. Lett. B **513**, 232 (2001) [[hep-ph/0105239](#)].
- [2] H. Georgi and A. Pais, Phys. Rev. D **10**, 539 (1974); Phys. Rev. D **12**, 508 (1975).
- [3] D. B. Kaplan and H. Georgi, Phys. Lett. B **136**, 183 (1984); Phys. Lett. B **145**, 216 (1984); D. B. Kaplan, H. Georgi and S. Dimopoulos, Phys. Lett. B **136**, 187 (1984); H. Georgi, D. B. Kaplan and P. Galison, Phys. Lett. B **143**, 152 (1984); M. J. Dugan, H. Georgi and D. B. Kaplan, Nucl. Phys. B **254**, 299 (1985).
- [4] N. Arkani-Hamed, A. G. Cohen, E. Katz and A. E. Nelson, JHEP **0207**, 034 (2002) [[hep-ph/0206021](#)].
- [5] N. Arkani-Hamed, A. G. Cohen, E. Katz, A. E. Nelson, T. Gregoire and J. G. Wacker, JHEP **0208**, 021 (2002) [[hep-ph/0206020](#)];
- [6] I. Low, W. Skiba and D. Smith, Phys. Rev. D **66**, 072001 (2002) [[arXiv:hep-ph/0207243](#)].

- [7] D. E. Kaplan and M. Schmaltz, JHEP **0310**, 039 (2003) [arXiv:hep-ph/0302049].
- [8] S. Chang and J. G. Wacker, Phys. Rev. D **69**, 035002 (2004) [arXiv:hep-ph/0303001].
- [9] W. Skiba and J. Terning, Phys. Rev. D **68**, 075001 (2003) [arXiv:hep-ph/0305302].
- [10] S. Chang, JHEP **0312**, 057 (2003) [arXiv:hep-ph/0306034].
- [11] M. Schmaltz, JHEP **0408**, 056 (2004) [arXiv:hep-ph/0407143].
- [12] P. Meade, arXiv:hep-ph/0402036.
- [13] C. Csaki, J. Hubisz, G. D. Kribs, P. Meade and J. Terning, Phys. Rev. D **67**, 115002 (2003) [arXiv:hep-ph/0211124].
- [14] J. L. Hewett, F. J. Petriello and T. G. Rizzo, JHEP **0310**, 062 (2003) [arXiv:hep-ph/0211218].
- [15] C. Csaki, J. Hubisz, G. D. Kribs, P. Meade and J. Terning, Phys. Rev. D **68**, 035009 (2003) [arXiv:hep-ph/0303236].
- [16] J. Wudka, arXiv:hep-ph/0307339.
- [17] H. C. Cheng and I. Low, JHEP **0309**, 051 (2003) [arXiv:hep-ph/0308199].
- [18] H. C. Cheng and I. Low, JHEP **0408**, 061 (2004) [arXiv:hep-ph/0405243].
- [19] I. Low, arXiv:hep-ph/0409025.
- [20] G. Burdman, M. Perelstein and A. Pierce, Phys. Rev. Lett. **90**, 241802 (2003) [Erratum-ibid. **92**, 049903 (2004)] [arXiv:hep-ph/0212228].
- [21] T. Han, H. E. Logan, B. McElrath and L. T. Wang, Phys. Rev. D **67**, 095004 (2003) [arXiv:hep-ph/0301040].
- [22] M. Perelstein, M. E. Peskin and A. Pierce, Phys. Rev. D **69**, 075002 (2004) [arXiv:hep-ph/0310039].
- [23] S. R. Coleman, J. Wess and B. Zumino, Phys. Rev. **177**, 2239 (1969). C. G. . Callan, S. R. Coleman, J. Wess and B. Zumino, Phys. Rev. **177**, 2247 (1969).
- [24] H. Georgi, “Weak Interactions And Modern Particle Theory,” 1985.
- [25] A. Birkedal-Hansen and J. G. Wacker, Phys. Rev. D **69**, 065022 (2004) [arXiv:hep-ph/0306161].
- [26] A. Pukhov *et al.*, arXiv:hep-ph/9908288.
- [27] A. Birkedal, K. Matchev and M. Perelstein, arXiv:hep-ph/0403004.
- [28] D. N. Spergel *et al.* [WMAP Collaboration], Astrophys. J. Suppl. **148**, 175 (2003) [arXiv:astro-ph/0302209].

- [29] H. C. Cheng, K. T. Matchev and M. Schmaltz, Phys. Rev. D **66**, 056006 (2002) [arXiv:hep-ph/0205314].
- [30] G. Azuelos *et al.*, arXiv:hep-ph/0402037.